the current gain to unity using a −6 dB/octave slope yields an f_t of 61 GHz for the 0·5 μm gate InGaAs MESFET. This high performance device is only conditionally stable with the stability factor K less than unity up to 25 GHz. The MSGs at 12, 18 and 25 GHz are 14·2, 12·4 and 11 dB, respectively. Measured under the same biasing conditions, the H_{21} and MSG for the 0·25 μm gate InGaAs MESFET is shown in Fig. 2. Extrapolation of the H_{21} gives a high f_t of 120 GHz. As the gate

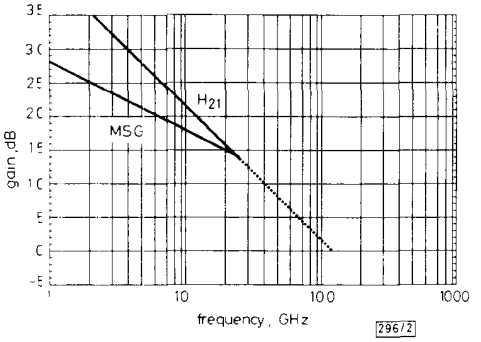

Fig. 2 *Current gain (H_{21}) and maximum stable gain (MSG) as a function of frequency for the 0·25 μm gate InGaAs MESFET*
f_T = 120 GHz

length is reduced to 0·25 μm, the MSGs at 12, 18, 25 GHz are significantly improved by roughly 3 dB to 17·3, 15·6 and 14·1 dB, respectively. Table 1 summarises and compares the microwave performance for the 0·5 μm and 0·25 μm gate devices. It is interesting to note that f_t increases by almost 100% when the gate length is reduced from 0·5 μm to 0·25 μm, as expected from the simple scaling rule, assuming the same average electron velocity for both devices. We would like to emphasise that these excellent microwave results are comparable or superior to those reported for 0·2 μm gate AlGaAs/InGaAs pseudomorphic HEMTs (f_t = 122 GHz) and 0·25 μm gate AlGaAs/InGaAs/GaAs quantum well MISFETs (f_t = 87 GHz).[3,4]

In summary, we show that InGaAs compounds are viable materials for MESFET devices, besides their more common application for HEMTs and MISFETs. State-of-the-art performance has been achieved using both 0·5 μm and 0·25 μm gate devices. With proper processing optimisation, the 0·25 μm gate devices show significant performance improvement over 0·5 μm gate devices.

G. W. WANG
M. FENG
R. KALISKI
Ford Microelectronics Inc.
9965 Federal Drive
Colorado Springs, CO 80921, USA

J. B. KUANG
School of Electrical Engineering
Cornell University
Ithaca, NY 14853, USA

22nd November 1989

References

1 WANG, G. W., CHEN, Y. K., RADULESCU, D. C., and EASTMAN, L. F.: 'A high-current pseudomorphic AlGaAs/InGaAs double quantum-well MODFET' *IEEE Electron Device Lett.*, 1988, **9**, pp. 4–6
2 WANG, G. W., FENG, M., KALISKI, R., LIAW, Y. P., LAU, C., and ITO, C.: 'Millimeter-wave ion-implanted graded $In_xGa_{1-x}As$ MESFET's grown by MOCVE', *IEEE Electron Device Lett.*, 1989, **10**, pp. 449–451
3 NGUYEN, L. D., RADULESCU, D. C., TASKER, P. J., SCHAFF, W. J., and EASTMAN, L. F.: '0·2 μm gate-length atomic-planar doped pseudomorphic $Al_{0.3}Ga_{0.7}As/In_{0.25}Ga_{0.75}As$ MODFET's with f_t over 120 GHz', *IEEE Electron Device Lett.*, 1988, **9**, pp. 374–376
4 KIM, B., MATYI, R. J., WURTLE, M., BRADSHAW, K., KHATIBZADEH, M. A., and TSERNG, H. Q.: 'Millimeter-wave power operation of an AlGaAs/InGaAs/GaAs quantum well MISFET', *IEEE Trans.*, 1989, **ED-36**, pp. 2236–2241
5 WANG, G. W., FENG, M., LAU, C. L., ITO, C., and LEPKOWSKI, T. R.: 'High performance millimeter-wave ion implanted GaAs MESFET's', *IEEE Electron Device Lett.*, 1989, **10**, pp. 95–97
6 MATTHEWS, J. W., and BLAKESLEE, A. E.: 'Defect in epitaxial multilayers, I. Misfit dislocation', *J. Cryst. Growth*, 1974, **27**, pp. 118–125
7 CAMACHO-PENALOSA, C., and AITCHISON, C. S.: 'Modeling frequency dependence of output impedance of a microwave MESFET at low frequency', *Electron. Lett.*, 1985, **21**, (12), pp. 528–529
8 KUANG, J. B., TASKER, P. J., WANG, G. W., CHEN, Y. K., EASTMAN, L. F., AINA, O. A., HIER, H., and FATHIMULA, A.: 'Kink effects in submicrometer-gate MBE-grown InAlAs/InGaAs/InAlAs heterojunction MESFET's', *IEEE Electron Device Lett.*, 1988, **9**, pp. 630–632

GAIN LIMITATION OF FIBRE RAMAN AMPLIFIERS CONSIDERING THIRD STOKES WAVELENGTH GENERATION

Indexing terms: Optical communications, Optical transmission

The use of a fibre Raman amplifier as a repeater amplifier and a power amplifier is studied by considering the third Stokes generation. Due to the multiple Stokes generation, there exists a limit on the achievable amplifier gain. With optimum pump powers, maximum amplifier gains of up to 58 dB and 28 dB are achievable for a repeater amplifier and a power amplifier, respectively.

Introduction: Optical amplification via stimulated Raman scattering in fibres, called fibre Raman amplifier (FRA), is attractive in fibre communication systems applications.[1–3] The FRA can be either used as a repeater amplifier at a repeating section to boost a weak signal, or adapted as a power amplifier at the transmitting end to increase the signal power to extend transmission distance. Under both conditions, if the pump power is strong enough to amplify the signal to a high power level, the signal may act as a source to generate high-order Stokes waves. In this letter we investigate the FRA used both as a repeater amplifier and a power amplifier by considering third Stokes wavelength generation. In usual Raman amplifications, the signal may be placed at the first or the second Stokes wavelengths of the pump. Here both cases are discussed.

Analysis: Consider a fibre system with transmission distance L. The pump power $P(0)$ and the Stokes powers $S_i(0)$, i = 1, 2, 3 denote the first, second and third Stokes wavelengths, respectively, are injected at $z = 0$ and propagate along the $+z$ direction. The coupled equations governing the pump and the Stokes propagations can be formulated as

$$\frac{dP(z)}{dz} = -\alpha_p P(z) - \frac{\lambda_{s1}}{\lambda_p}\frac{g_0}{A} S_1(z)P(z) \quad (1)$$

$$\frac{dS_1(z)}{dz} = -\alpha_{s1} S_1(z) + \frac{g_0}{A} S_1(z)P(z) - \frac{\nu_{s2}}{\nu_{s1}}\frac{g_1}{A} S_2(z)S_1(z) \quad (2)$$

$$\frac{dS_2(z)}{dz} = -\alpha_{s2} S_2(z) + \frac{g_1}{A} S_2(z)S_1(z) - \frac{\nu_{s3}}{\nu_{s2}}\frac{g_2}{A} S_3(z)S_2(z) \quad (3)$$

$$\frac{dS_3(z)}{dz} = -\alpha_{s3} S_3(z) + \frac{g_2}{A} S_3(z)S_2(z) \quad (4)$$

where α_i and λ_i ($i = p, s1, s2, s3$) are the fibre loss coefficients and the wavelengths of the pump, as well as the three Stokes waves. A is the effective Raman cross-section, which is

assumed to be the same for the various Stokes waves. g_j, $j = 0, 1, 2$, denote the Raman gain constant of the three Stokes generations, respectively. Here, the polarisation of the fibre is assumed to be maintained.[4]

Let the input signal power be much larger than the spontaneous emission power. Then the three input Stokes powers can be determined in two ways. If the Stokes wavelength has signal input, then its input power is equal to the injected signal power. On the other hand, if the Stokes wavelength has no signal input, its input power is taken as an equivalent spontaneous emission power, which is equal to 1 nW in our examples. Thus the initial Stokes powers at $z = 0$ are available. The pump and the three Stokes powers along the fibre can be obtained by numerically solving the coupled equations. We at first consider the case where the signal is located at the first Stokes wavelength. This is the common case in FRA applications because the pump power can be directly coupled to the signal. One of the examples of the propagation of the four waves is shown in Fig. 1. We see that the signal S_1 is at

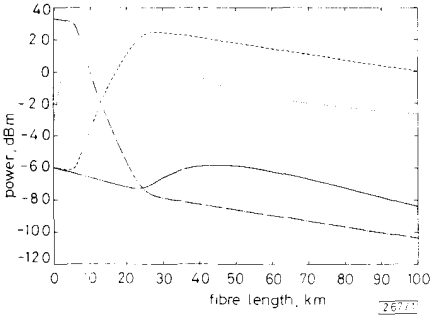

Fig. 1 *Signal and pump power variation against fibre length*

$P(0) = 2$ W, $S_1(0) = 1\,\mu$W, $S_2(0) = 1$ nW, $S_3(0) = 1$ nW, $A = 5 \times 10^{-11}$ m^2, $\lambda_p = 1{\cdot}45\,\mu$m, $\lambda_{s1} = 1{\cdot}55\,\mu$m, $\lambda_{s2} = 1{\cdot}67\,\mu$m, $\lambda_{s3} = 1{\cdot}8\,\mu$m, $\alpha_p = 0{\cdot}35$ dB/km, $\alpha_{s1} = 0{\cdot}2$ dB/km, $\alpha_{s2} = 0{\cdot}35$ dB/km, $\alpha_{s3} = 0{\cdot}6$ dB/km, $g_0 = g_1 = g_2 = 7{\cdot}5 \times 10^{-14}$ m/W
—·— $P(z)$ ····· $S_1(z)$ – – – – $S_2(z)$ —— $S_3(z)$

first amplified by the pump to a high power level and then acts as a pumping source to amplify the second Stokes wavelength. With the generation of the second Stokes wavelength, the signal power is seriously depleted. The second Stokes, after it has been pumped to a high power level, again acts as another source to amplify the third Stokes wavelength. Since the power level of the second Stokes wavelength is not high enough, the third Stokes wavelength is only partially amplified.

Discussion We define the amplifier gain of the signal as

$$G = 10 \log \frac{S_1(L)}{S_1(0)e^{-\alpha_{s1}L}} \tag{5}$$

where $S(L)$ is the signal power at $z = L$. The amplifier gain as a function of pump power for a repeater amplifier ($S_1(0) = 1\,\mu$W) and a power amplifier ($S_1(0) = 1$ mW) is shown in Fig. 2. We find that there exists an optimum power to achieve a maximum amplifier gain, which does not occur if only first Stokes radiation is considered.[1] When the pump power increases beyond the optimum value, the amplified signal is strong enough to generate a strong second Stokes wavelength, the depleted power due to the second Stokes becomes larger than that obtained from the increased pump power, so the gain decreases. We see that an amplifier gain of up to 58 dB can be obtained when the FRA is used as a repeater amplifier with 1·5 W pump power. In comparison 28 dB gain is available for a power amplifier, with a lower pump power. We next consider the case where the signal is located at the second Stokes wavelength of the pump. This may occur if the pump source is not available to produce first Stokes at the signal wavelength. The amplifier gain can be defined similarly to eqn. 5 by replacing the subscript 1 with 2. Fig. 3 shows the amplifier gain as a function of pump power. For $P(0) < 1$ W, there is no amplifier gain because the first Stokes is not large enough to amplify the signal. For $1\,\text{W} < P(0) < 1{\cdot}5\,\text{W}$, which can be

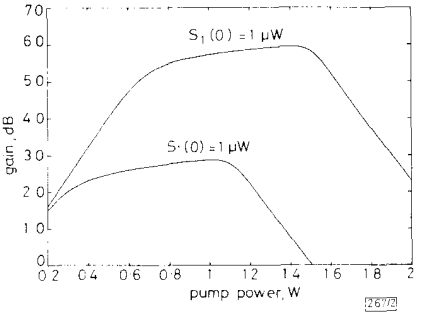

Fig. 2 *Amplifier gain as a function of pump power*

$S_2(0) = 1$ nW, $S_3(0) = 1$ nW. System parameters as Fig. 1

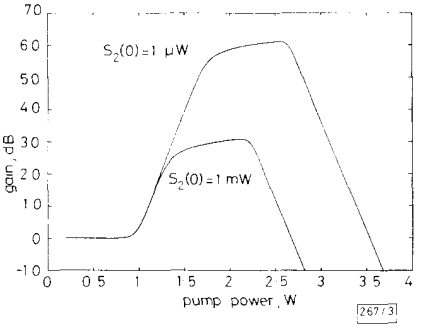

Fig. 3 *Amplifier gain as a function of pump power*

$S_1(0) = 1$ nW, $S_3(0) = 1$ nW, $\lambda_p = 1{\cdot}36\,\mu$m, $\lambda_{s1} = 1{\cdot}45\,\mu$m, $\lambda_{s2} = 1{\cdot}55\,\mu$m, $\lambda_{s3} = 1{\cdot}67\,\mu$m, $\alpha_p = 0{\cdot}3$ dB/km, $\alpha_{s1} = 0{\cdot}35$ dB/km, $\alpha_{s2} = 0{\cdot}2$ dB/km, $\alpha_{s3} = 0{\cdot}35$ dB/km

characterised as the linear gain region, the amplified first Stokes power becomes high enough to amplify the signal such that the amplifier gain increases linearly with the pump power. For $P(0) > 1{\cdot}5$ W, the gain begins to saturate and increases at a much slower rate with the pump power. After reaching a maximum value, the amplifier gain decreases as the pump power further increases because the generation of the third Stokes wavelength may deplete more power from the signal than it obtained from the increased pump power. The maximum achievable amplifier gain is about the same as those in Fig. 2, but a higher pump power must be used.

Conclusion: In this letter we investigate fibre Raman amplification by considering third Stokes wavelength generation. The results show that there exists a limitation on the achievable amplifier gain owing to the generation of high-order Stokes radiation. We have studied the application of the FRA both as a repeater amplifier and a power amplifier and maximum amplifier gains up to 58 dB and 28 dB are achievable, respectively. We also see that the maximum amplifier gain is the same whether the signal is located at the first or the second Stokes wavelength. However, higher pump power should be used to achieve the same amplifier gain if the signal is located at the second Stokes wavelength.

M.-S. KAO
J. WU

Department of Electrical Engineering
National Taiwan University
Taipei, Taiwan 10764, Republic of China

17th November 1989

References

1 MOCHIZUKI, K.: 'Optical fiber transmission systems using stimulated Raman scattering theory', *J. Lightwave Technol.*, 1985, **3**, pp. 688–694

2 AOKI, Y.: 'Properties of fiber Raman amplifiers and their applicability to digital optical communication systems', *J. Lightwave Technol.*, 1988, **6**, pp. 1225–1239
3 KAO, M. S., and WU, J.: 'Signal light amplification by using stimulated Raman scattering in a N-channel WDM optical fiber communication system', *J. Lightwave Technol.*, 1989, **7**, pp. 1290–1299
4 STOLEN, R. H.: 'Polarization effects in fiber Raman and Brillouin lasers', *IEEE J.*, 1979, **QE-15**, pp. 1157–1160

EPITAXIAL LIFT-OFF GaAs LEDs TO Si FOR FABRICATION OF OPTO-ELECTRONIC INTEGRATED CIRCUITS

Indexing terms: Integrated circuits, Optoelectronics, Silicon, Lithography

We report, for the first time, the successful integration of GaAs LEDs on Si using the epitaxial lift-off technique. LEDs were processed after the transfer and could be aligned to features on the Si substrate. LED contacts were defined on both sides of the thin layer. Operation characteristics similar to those of LEDs grown on GaAs were observed. This realisation holds out interesting prospects in the fabrication of quasi-monolithic opto-electronic integrated circuits.

Introduction: In recent years, there has been an increasing interest in the integration of III-V semiconductors with Si. This material combination is important in the realisation of opto-electronic integrated circuits (OEICs) which finds many applications in broadband and coherent optical communication networks and in optical printing and recording. This integration was, up to now, mainly achieved in a hybrid or with the flip-chip technique.[1] Research is also going on into the monolithic integration of III-V devices on Si with lattice mismatched hetero-epitaxial growth.[2] In this paper, we describe a quasi-monolithic integration using the epitaxial lift-off technique (in brief epi-lift-off or ELO).[3] In this new approach, GaAs epitaxial layers can be lifted off from GaAs substrates by means of a very selective etch of an underlying AlAs layer. The thin epilayers can then be attached to arbitrary substrates, e.g. Si, glass, $LiNbO_3$, InP, etc., without significant degradation of the epilayer quality.

There are two approaches which can be used to realise the quasi-monolithic integration: (*a*) devices can be fully processed before ELO and then transferred to an arbitrary substrate; or (*b*) unprocessed ELO layers can be attached to any substrate and can then be processed and interconnected with other devices on the substrate. Most effort has been concentrated on the first approach,[4,5] and in this way we realised e.g. the successful transfer of MESFETs to InP,[6] LEDs to Si,[7] and MQW optical modulators to glass. Several problems are present in this option, e.g. the alignment to substrate circuits and the strain induced by dielectrics and metallisations. The second approach, to which far less attention is paid,[8] has the advantages that thin ELO layers can be attached with sufficient strength for further processing, and that no process incompatibilities occur during the processing of the ELO and/or substrate devices. The problem of alignment is not present because photolithographical masks can be aligned to substrate features. Strain problems can also be reduced when metallisations and dielectrics are deposited after the layer transfer.

This letter is concerned with the second approach and describes for the first time the successful integration of GaAs LEDs, fully processed after ELO transfer, on a Si substrate. LED contacts were present on both sides of the ELO layer and the backside contact was electrically interconnected with a metallisation on the Si substrate. The ELO LEDs on Si were comparable with LEDs on GaAs and showed much better performances than similar LEDs grown directly on Si.[9]

Device fabrication: The epitaxial structure, shown in Fig. 1, was grown using metal organic vapour phase epitaxy (MOVPE) on a GaAs substrate. The LED epilayers were lifted off their GaAs substrate using a wax carrier and a

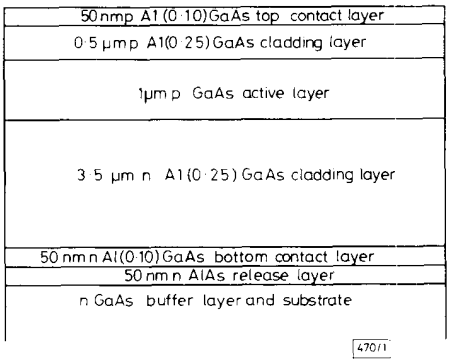

Fig. 1: *Schematic representation of the LED layer structure grown by MOVPE*

HF : H_2O (1 : 5) solution at 0°C. An AuGe/Ni backside metallisation was then deposited on the released side. After the wax was removed from the other side, the ELO layers were mounted with a silver epoxy in channels in a Si substrate. The channels were photolithographically defined, etched in a KOH : isopropylalcohol solution, and then covered with an AuGe/Ni metallisation. After the silver epoxy was hardened by a bake-out, the ELO layer was sufficiently well attached for further processing, which used conventional processes involving optical lithography. The masks that were used in all steps could be aligned to features on the Si substrate. First, a Zn/Au metallisation pattern was deposited, followed by a fast alloying step at 420°C to obtain ohmic contacts on both sides of the thin layers. Next, an additional TiW/Au cap was deposited on the bonding pads and a mesa etch with $H_2SO_4 : H_2O_2 : H_2O$ (1 : 1 : 18) was finally used to isolate the different LEDs.

Results and discussion: A top view of the final structure is shown in Fig. 2. Since our aim was to show the feasibility of

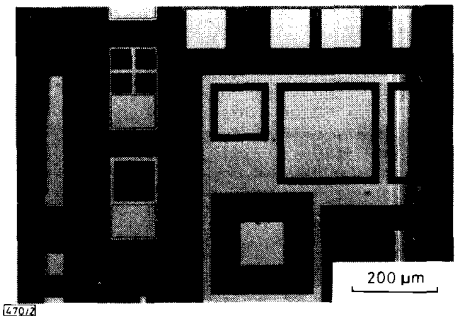

Fig. 2 *GaAs ELO layer, fully processed after the transfer to a Si substrate*

processing-after-lift-off, we used a standard all-purpose mask set which was not designed to the ELO layer dimensions and which contained several LED structures. A one-window and a four-window LED, for example, are shown on the left-hand side of the picture. Since a planar structure was obtained before the LED processing, it was possible to realise photolithographical patterns on the ELO film with nearly no distortion even at the edges of the layer. Operating characteristics were compared to those of LEDs fully processed on GaAs. The layer structure of these LEDs was identical to that in Fig. 1 including the AlAs layer. In Fig. 3 output power (normalised to one steradial) against input current characteristics are compared and, as can be seen, slightly more output power was obtained with LEDs processed on the ELO layer. The difference can be explained in terms of processing variations, or perhaps beneficial effects induced by the ELO technique.